THE JOURNAL OF BIOLOGICAL CHEMISTRY
Vol. 272, No. 36, Issue of September 5, pp. 22502–22508, 1997

Printed in U.S.A.

Studies on the Redox Centers of the Terminal Oxidase from *Desulfovibrio gigas* and Evidence for Its Interaction with Rubredoxin*

(Received for publication, April 22, 1997, and in revised form, June 30, 1997)

Cláudio M. Gomes‡, Gabriela Silva‡§, Solange Oliveira§, Jean LeGall‡¶, Ming-Yih Liu¶, António V. Xavier‡, Claudina Rodrigues-Pousada§, and Miguel Teixeira‡‖

From the ‡Instituto de Tecnologia Química e Biológica, Universidade Nova de Lisboa, Oeiras, Portugal, the §Instituto Gulbenkian de Ciência, Laboratório de Genética Molecular, Oeiras, Portugal, and the ¶Department of Biochemistry and Molecular Biology, University of Georgia, Athens, Georgia 30602

Rubredoxin-oxygen oxidoreductase (ROO) is the final component of a soluble electron transfer chain that couples NADH oxidation to oxygen consumption in the anaerobic sulfate reducer *Desulfovibrio gigas*. It is an 86-kDa homodimeric flavohemeprotein containing two FAD molecules, one mesoheme IX, and one Fe-uroporphyrin I per monomer, capable of fully reducing oxygen to water. EPR studies on the native enzyme reveal two components with g values at ~2.46, 2.29, and 1.89, which are assigned to low spin hemes and are similar to the EPR features of P-450 hemes, suggesting that ROO hemes have a cysteinyl axial ligation. At pH 7.6, the flavin redox transitions occur at 0 ± 15 mV for the quinone/semiquinone couple and at −130 ± 15 mV for the semiquinone/hydroquinone couple; the hemes reduction potential is −350 ± 15 mV. Spectroscopic studies provided unequivocal evidence that the flavins are the electron acceptor centers from rubredoxin, and that their reduction proceed through an anionic semiquinone radical. The reaction with oxygen occurs in the flavin moiety. These data are strongly corroborated by the finding that rubredoxin and ROO are located in the same polycistronic unit of *D. gigas* genome. For the first time, a clear role for a rubredoxin in a sulfate-reducing bacterium is presented.

Despite the fact that they are still being considered as *strict anaerobes*, sulfate reducing bacteria when exposed to oxygen are capable of surviving (1, 2) as well as of taking advantage of its presence in terms of energy conservation (3, 4). In the presence of oxygen, the sulfate reducer *Desulfovibrio gigas*, uses internal reserves of polyglucose, which is metabolized by the Embden-Meyerhof-Parnas pathway thus generating NADH and ATP (3). In this bacterium a three-component soluble electron transfer chain couples NADH oxidation with oxygen reduction to water, allowing simultaneously for NAD^+ regeneration and oxygen utilization. The proteins involved are NADH:rubredoxin oxidoreductase (NRO)[1] (5), rubredoxin (Rd) (6), and rubredoxin:oxygen oxidoreductase (ROO) (7), as shown in Scheme I.

NRO, the first component of this pathway, contains two subunits of 27 and 32 kDa and is a flavoprotein containing four flavin groups (FMN and FAD) per molecule with reduction potentials (Fl_{ox}/Fl_{red}) of −295 and −325 mV, at pH 7.6. This NADH oxidase reduces *D. gigas* Rd, a 6-kDa iron protein, with a reduction potential of 0 ± 5 mV. NRO is highly specific toward this redox protein (5). *D. gigas* desulforedoxin (8), *Desulfovibrio desulfuricans* Rd (9), or even *Desulfovibrio vulgaris* Rd (10) are hardly reduced by NRO (5), despite the similarity between the reduction potentials of these proteins. *D. gigas* Rd was also found to be necessary for the coupling of NRO to the final component of the chain, ROO (7). This enzyme can be seen as a true terminal oxidase since it is capable of catalyzing the four-electron reduction of oxygen to water without the formation of partially reduced oxygen species (7). It is an 86-kDa homodimeric flavohemeprotein, containing two FAD and two distinct hemes per monomer. These hemes are of unusual types: uroporphyrin I and a noncovalently bound derivative of mesoheme IX (7, 11). Finding the type I Fe-uroporphyrin isomer, so far considered as a non-metabolite that accumulates in some genetically linked porphyrias, in a physiologically active enzyme is unprecedented and raises the possibility that uroporphyrin I may be of physiological importance in other organisms.

Preliminary studies of this system suggested the involvement of rubredoxin in a physiological reaction in a strict anaerobe (7). However, its direct reaction with the terminal oxidase remained to be demonstrated. In the present study, the redox centers of this so far unique enzyme are characterized spectroscopically as well as in terms of their reduction potentials. The electron transfer between the components of *D. gigas* oxygen-utilizing pathway is probed by EPR and visible spectroscopy. Unequivocal spectroscopic evidence for the direct involvement of Rd in the electron transfer to ROO is provided. Also, using genetic approaches, we show that the Rd is located in the same polycistronic unit of the ROO coding region.

EXPERIMENTAL PROCEDURES

Bacterial Strains and Plasmids—D. gigas (ATCC 19364) was grown as described previously (12). *Escherichia coli* strain LE 392, and *E. coli* P2 392 were used to screen the genomic library and in the purification of the recombinant positive phages. Competent cells of *E. coli* XL2-Blue

* This work was supported by Praxis XXI (Praxis/2/2.1/Bio/20/94 and 1075/95) and European Commission Grants Bio4-CT96-0413 and ERBCHRXCT940626 (to M. T.), National Institutes of Health Grant GM56001-01 (to J. L. G. and M. Y. L.), Fundaçaõ Calouste Gulbentian grants (to C. R. P.), and Programa Gulbentian Doutoramento em Biologia e Medicina and Praxis XXI (BD9793/96) (to C. G.) and Praxis XXI (BD9016/96) (to G. S.). The costs of publication of this article were defrayed in part by the payment of page charges. This article must therefore be hereby marked "*advertisement*" in accordance with 18 U.S.C. Section 1734 solely to indicate this fact.

‖ To whom correspondence should be addressed. Tel.: 351-1-442-62-46; Fax: 351-1-442-87-66; E-mail: miguel@itqb.unl.pt.

[1] The abbreviations used are: NRO, NADH:rubredoxin oxidoreductase; ROO, rubredoxin-oxygen oxidoreductase; Rd, rubredoxin; Fl_{ox}, flavin quinone; Fl_{sq}, flavin semiquinone; Fl_{red}, flavin hydroquinone; ORF, open reading frame; mT, millitesla.

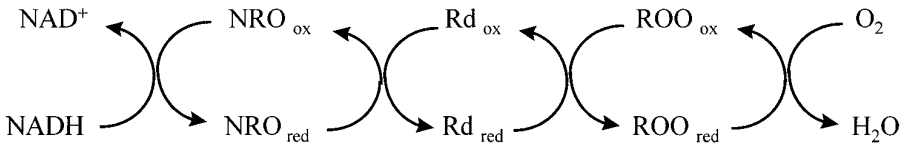

SCHEME 1.

Cells (Stratagene) and/or *E. coli* TOP 10F′ (Invitrogen), prepared according to standard protocols (13), were used to transform the DNA fragments subcloned into the polylinker of the plasmid pZErO™-1 (Invitrogen).

Preparation of Genomic DNA—Genomic DNA isolated from *D. gigas* was extracted as described (14). Plasmid DNA was prepared using the plasmid purification kit Qiagen (Diagen).

Cloning of Rd and ROO—Degenerate primers (5′-ATGCARGCRACRAARATHAT-3′ and 5′-TTRTAYGTYGTYCCCATYGG-3′) of both extremities of the amino acid sequence corresponding to the N terminus of ROO were used to amplify genomic DNA. The polymerase chain reaction cycling conditions were: 5 cycles at 94 °C for 30 s, 40 °C for 60 s, and 72 °C for 30 s followed by 30 cycles at 92 °C for 30 s, 48 °C for 30 s, 72 °C for 30 s, and finally 72 °C for 10 min. The reaction product with 106 base pairs was then subcloned in pZErO™-1 and sequenced (see below). This procedure allowed us to obtain a homologous probe which was labeled with [α-^{32}P]dATP using the megaprime DNA labeling system (Amersham). This probe was used to screen a *Sau*3A1 genomic library from *D. gigas* constructed in λ Dash II as vector (Stratagene). Filters were prehybridized and hybridized at 55 °C with 6 × SSC (SSC, 0.15 M NaCl, 15 mM trisodium citrate, pH 7.0), 5 × Denhardt's solution, 0.5% SDS (mass/volume), 200 μg/ml sonicated salmon sperm DNA. The filters were washed using 2 × SSC, or 2 × SSC with 0.2% SDS at the hybridization temperature. The washings were performed at a temperature higher than 55 °C, depending on the intensity of the signal.

Positive phages were purified and their DNA isolated according to the technique described as in Ref. 15. The DNA was then digested with *Bam*HI, and the fragments corresponding to a size of 3.6 kilobases were subcloned into pZErO™-1.

DNA Sequencing—Suitable restriction fragments were subcloned in pZErO™-1 and sequenced using the Termo Sequenase cycle sequencing kit according to the supplier's instructions (Amersham). This procedure was used to solve the compressions, as the *D. gigas* genome has a high G + C content (16). Sequential deletions were also made using the double-stranded Nested Deletion kit (Pharmacia).

Protein Purification—*D. gigas* soluble extract was prepared as described (12). ROO was purified essentially according to Ref. 7 but an extra purification step was performed after the last gel filtration column. The ROO-containing fraction from this column was dialyzed overnight against 10 mM Tris-HCl, pH 7.6, buffer and applied on a Pharmacia Mono-Q FPLC column. A 10–500 mM gradient of the same buffer at 0.5 ml min^{-1} was applied; pure ROO eluted at ~75 mM ionic strength. Typical yields are 4–7 mg of ROO/kg of cell mass (wet weight). NRO and Rd were prepared by the procedures of Refs. 5 and 17, respectively. The protein was judged pure by SDS-polyacrylamide gel electrophoresis which showed a single band at 43 kDa.

Protein Quantitation and Analysis—The protein N-terminal sequence was determined using an Applied Biosystem Model 470A sequenator. Search of protein sequences showing homology with the N terminus was performed at the NCBI using the BLAST network service. The protein concentration was determined by the method of Bradford (18).

Spectroscopic Methods—Room temperature ultraviolet/visible spectra were recorded in a Beckman DU-70 spectrometer. Visible redox titrations were performed in a Shimadzu spectrometer (UV 265) equipped with a cell stirring system. Low temperature (77 K) visible spectra were recorded on a DW-2 OLIS spectrophotometer. EPR spectra were recorded as in Ref. 19. The EPR spectra obtained under nonsaturating conditions were integrated using the Aasa and Vänngård (20) correction factor. Myoglobin azide (1.2 mM) was used as a standard (21). Fluorescence spectra were taken in a SPEX Fluorolog 212.

Redox Titrations—ROO (1.5 μM) was titrated anaerobically in 50 mM Tris-HCl, pH 7.6, by stepwise addition of buffered sodium dithionite. The following compounds were used as redox mediators (0.25 μM each): methylene blue (E'_0 = 11 mV), indigo tetrasulfonate (E'_0 = −30 mV), indigo trisulfonate (E'_0 = −70 mV), indigo disulfate (E'_0 = −182 mV), antraquinone 2,7-disulfonate (E'_0 = −182 mV), safranine (E'_0 = −280 mV), neutral red (E'_0 = −325 mV), benzyl viologen (E'_0 = −359 mV), and methyl viologen (E'_0 = −446 mV). The reduction potentials are quoted *versus* the standard hydrogen electrode.

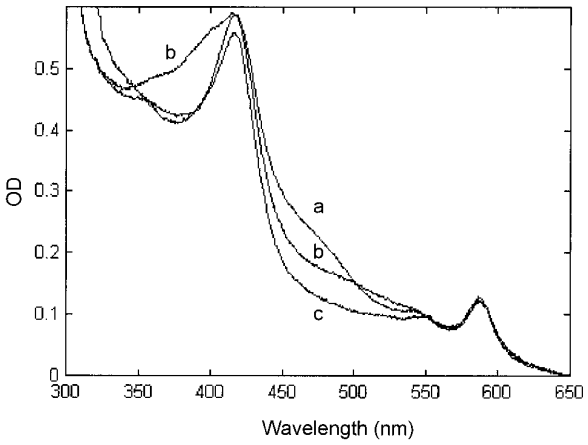

FIG. 1. **UV-visible spectra of ROO in several redox states.** *Trace a,* as prepared ROO (1.5 μM) in 50 mM Tris-HCl buffer, pH 7.6; *traces b* and *c,* partially reduced samples with dithionite. Only 3 out of 46 spectra from a titration in the absence of redox mediators are shown.

The experimental data were manipulated and analyzed using MATLAB (Mathworks, South Natick, MA) for Windows. Spectral smoothing and optical deconvolution was performed using singular value decomposition in combination with a curve fitting algorithm (22).

RESULTS

Spectroscopic Characterization—The UV-visible spectrum of native ROO is dominated by a Soret band at 416 nm due to the hemes, a flavin contribution in the 460-nm region and a distinctive feature at 587 nm whose origin is unclear (Fig. 1, *trace a*). The spectra are similar both when recorded at 77 K and at room temperature. A red flavin semiquinone species accumulates transiently during reduction, as detected at 480 and 380 nm (Fig. 1, *trace b*). In the fully reduced enzyme, α and β bands are present at 551 and 522 nm, respectively (*cf.* Fig. 5*A*). Moreover, the Soret nor the 587-nm bands shift (7). The interaction of native ROO with exogenous ligands, such as cyanide, cysteine, dithiothreitol, and mercaptoethanol was studied. However, no spectral changes were observed, even upon rather extensive incubation periods (data not shown).

Fluorescence excitation and emission spectra of native ROO only revealed the characteristic fingerprint of the flavin moiety (Fig. 2) (23). The emission spectrum, obtained with the excitation at 416 nm gives a single band at 527 nm. The excitation spectrum, with the emission wavelength at 520 nm, shows bands at 373 and 464 nm with a shoulder at 342 nm. No emission was obtained with excitation at 587 nm. The emission spectra of ROO is similar to those of free FAD and FMN, *D. gigas* flavodoxin,[2] and ferredoxin-NADP$^+$ oxidoreductase (24). Since there is a different degree of exposure to the solvent of the isoalloxazine rings in flavodoxins (25) and in FNR (26), nothing can be concluded about the flavin environment in ROO on the basis of its fluorescence characteristics.

The EPR spectra of ROO present some rather unique characteristics (Fig. 3). The spectra are dominated by resonances at g ~2.46, 2.29, and 1.89, which appear to result from two rhom-

[2] C. M. Gomes, J. LeGall, A. V. Xavier, and M. Teixeira, unpublished observations.

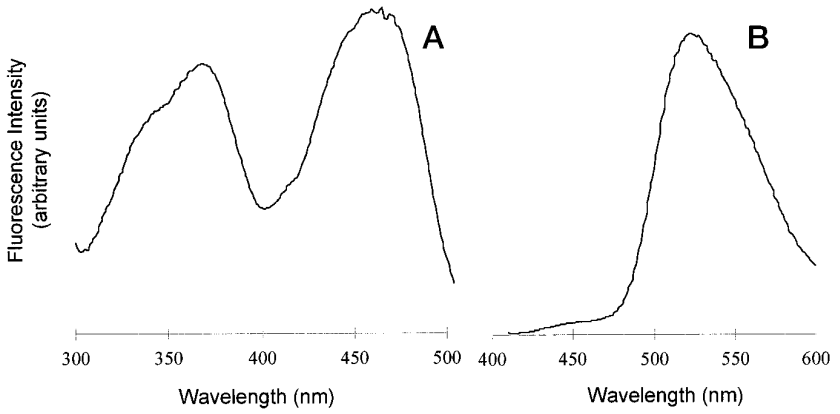

FIG. 2. **Excitation (*a*) and emission (*b*) spectra of *D. gigas* ROO.** Native ROO (1.5 μM) in 50 mM Tris-HCl buffer, pH 7.6. The excitation spectra was recorded with the emission wavelength set at 520 nm and the emission spectra was recorded with excitation at 416 nm.

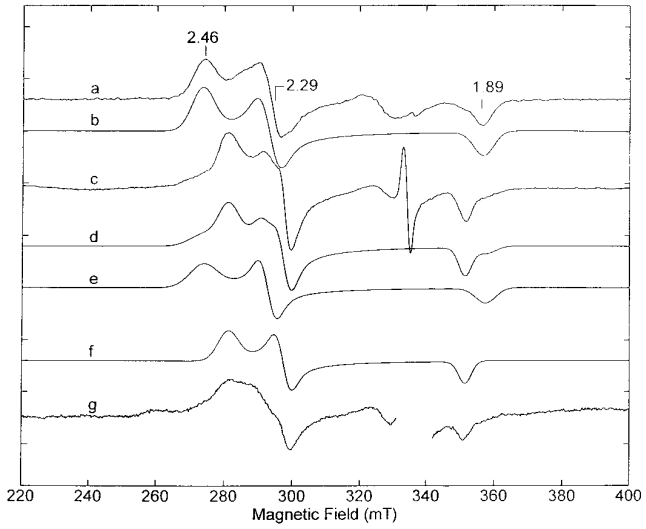

FIG. 3. **EPR spectra of *D. gigas* ROO as prepared and in the presence of NADH, NRO, and Rd.** *Traces a* and *c*, native ROO, two different preparations; *trace b*, theoretical simulation of trace *a* with $g_{1,2,3}$ = 2.467, 2.300, 1.890 and line widths $w_{1,2,3}$ = 8.0, 6.5 and 7.0 mT; *trace d*, simulation of *trace c*, obtained by adding two components with $g_{1,2,3}$ = 2.401, 2.270, 1.920 (*trace e*, $w_{1,2,3}$ = 7.0, 4.8, and 4.5 mT) and $g_{1,2,3}$ = 2.467, 2.305, 1.887 (*trace f*, $w_{1,2,3}$ = 9.5, 5.0, and 7.0 mT); *trace g*, spectrum of ROO (3 times diluted) after addition of NRO (1 μM), Rd (1 μM), and NADH (5 mM). In the g = 2 region a strong radical signal was eliminated for clarity. Temperature: 24 K, microwave power: 2.4 mW, microwave frequency, 9.44 GHz, modulation amplitude, 1 mT.

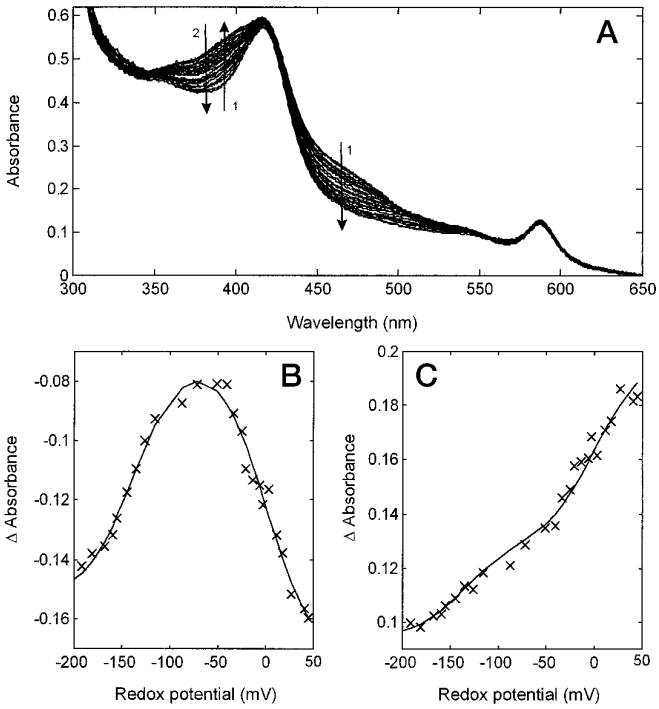

FIG. 4. **Visible redox titration of ROO flavins.** *Panel A*, visible spectra of ROO (1.5 μM) obtained along the redox titration varying the potential from 49 to −196 mV. *Arrows* and *numbers* indicate, respectively, the direction and sequence of the changes; *panel B*, titration curve of the flavins followed at 380–416 nm; *panel C*, titration curve of flavins followed at 460–565 nm. The *lines* in *panels B* and *C* correspond to a fitting to the sequential equilibrium $Fl_{ox} \ll Fl_{sq} \ll Fl_{red}$, with E_1 = 0 mV and E_2 = −130 mV, n = 1.

bic components, as deduced from the comparison and theoretical simulations of the spectra obtained from several ROO preparations. The g values and line shapes observed are slightly variable among different sample preparations, but nonetheless the main characteristics are common to all preparations so far studied. These signals are optimally detected at around 40–50 K, but are still observable, without noticeable line broadening due to the increase of the electronic relaxation time, up to at least 200 K. The intensities of these signals also vary from preparation to preparation. A maximum of 2 spins per monomer were determined from double integration of both the experimental and theoretically simulated spectra, obtained under nonsaturating conditions. Due to these values, as well as to the g values observed, which are similar to those of P-450 enzymes (27–29), these resonances were assigned to the two ROO heme groups. Since the spectral features remain unaltered in a broad temperature range (20–200 K for EPR and 77–298 K for visible spectroscopy), it may be concluded that they are low-spin in this entire temperature range. Two other low intensity resonances are also observed in some samples: a minor component at g ~ 6, characteristic of high-spin hemes, and a radical type signal at g ~ 2.0, with a line width of 1.6 mT, identical to those observed in flavin red semiquinones (49).

Upon incubation of ROO with NADH, NRO and Rd the intensity of the radical signal at g ~ 2 increases, which is likely to be due to the stabilized semiquinone radical of the FAD. The rhombic spectra are essentially unaltered, except for an overall line broadening and a slight g value shift (Fig. 3, *trace g*). These results strongly suggest that the hemes are not reduced by the redox chain NADH/NRO/Rd. Upon reduction with sodium dithionite an EPR silent state is obtained. Although the 587-nm band as well as the intensity of the EPR signals of purified ROO vary slightly among preparations, these variations are not reflected in the catalytic activity of ROO.

Redox Properties of ROO—Preliminary studies were performed in the absence of redox mediators (Fig. 1, only 3 out of 46 spectra are shown). These data show that it is possible to follow independently the flavin and heme centers, that the two

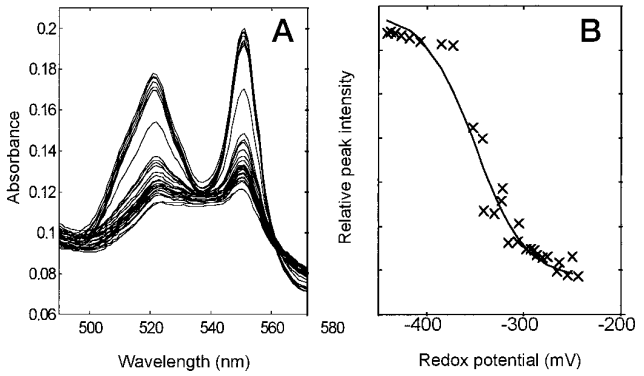

FIG. 5. **Visible redox titration of ROO hemes.** *Panel A*, visible spectra of ROO obtained along the redox titration varying the potential from −250 to −449 mV. *Panel B*, titration curve of ROO hemes followed at 550 nm, corrected in respect to 565 and 535 nm isosbestic points. The *line* corresponds to a Nernstian process, $E_m = -350$ mV, $n = 1$.

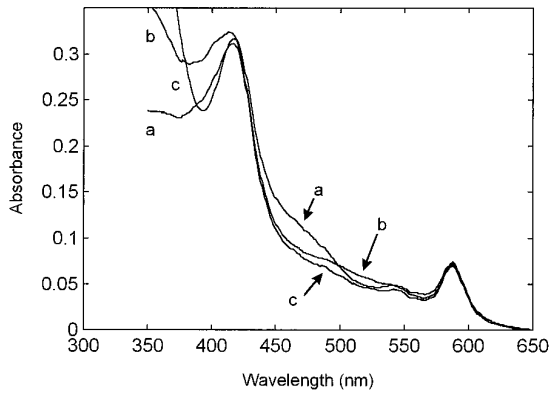

FIG. 6. **Reduction of ROO flavins by NADH, NRO, and Rd.** ROO (2 μM) was in 50 mM Tris-HCl buffer, pH 7.6. *Trace a*, after addition of NRO (2.5 nM) and NADH (4 μM); *trace b*, recorded 1 min after further addition of Rd (3 μM); *trace c*, recorded after 60 min of incubation.

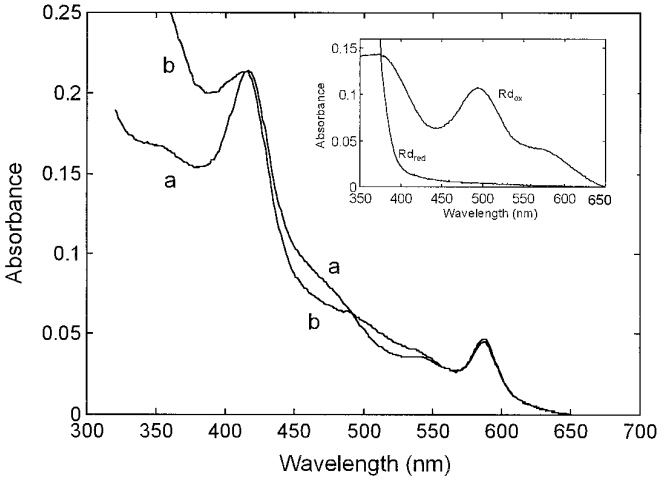

FIG. 7. **Interaction between reduced Rd and ROO.** ROO (1.5 μM) was in 50 mM Tris-HCl buffer, pH 7.6. *Inset,* 16 μM oxidized Rd (Rd_{ox}) was incubated anaerobically with 160 μM NADH and 3 nM NRO. After 5 min, full reduction was achieved (Rd_{red}). *Trace a*, native ROO; *trace b*, 1 min after addition of reduced Rd (2 μM).

flavins are equivalent and have a reduction potential higher than the hemes, and that flavin reduction occurs in two sequential processes through a red anionic type semiquinone intermediate.

The reduction potentials of ROO flavins were determined from two independent visible titrations (Fig. 4, *panel A*). Large spectral changes occur at 460 nm (oxidized flavin decay) and at 380 and 480 nm (appearance and disappearance of the flavin semiquinone). Since absorbance does not change at 416 and 565 nm, the variations of absorbance at 380–416 nm (Fig. 4, *panel B*) and 460–565 nm (Fig. 4, *panel C*) were plotted against the redox potential. Fitting the data to two sequential Nernst processes yielded the following reduction potentials: 0 ± 15 mV (Fl_{ox}/Fl_{sq}) and −130 ± 15 mV (Fl_{sq}/Fl_{red}). Singular value decomposition analysis of the data confirmed these results. The deconvolution of the optical species yielded a spectral component which was assigned to the red flavin semiquinone. The fitted reduction potentials were similar to those obtained by conventional analysis (data not shown). From the reduction potentials determined, the expected intensity of the semiquinone species for a sequential redox process would be 0.88, in good agreement with the theoretical value of 0.73 calculated based upon the extinction coefficients of quinone and red semiquinone at 385 nm (23).

The data previously obtained (11) indicated that both the low-spin mesoheme and iron uroporphyrin I have identical α and β bands in the protein, as well as similar pyridine hemochrome spectra. In agreement with this fact, ROO hemes could not be resolved spectroscopically along the redox titration (Fig. 5, *panel A*). Their reduction potential was determined to be −350 ± 10 mV, following the increase in the absorbance of these two bands, in two independent titrations (Fig. 5, *panel B*).

Probing for Direct Interaction of Rd with ROO—By visible spectroscopy no spectral changes are observed upon anaerobic incubation of ROO with NADH and NRO (Fig. 6, *trace a*), confirming that ROO is not directly reduced by either NADH or NRO. After addition of oxidized Rd, the ROO flavins are reduced. In a short time period (1 min) after addition, the flavin semiquinone species accumulates (Fig. 6, *trace b*); this species then decays to the fully reduced flavin, as seen by the complete bleaching at 460 nm and the disappearance of the 380-nm band within the next minutes (Fig. 6, *trace c*). Further incubation does not result in heme reduction. Adding air-saturated buffer to the mixture causes immediate reoxidation of the flavins. As described above, a similar experiment followed by EPR, showed also that anaerobic incubation of ROO with NRO and Rd does not result in the disappearance of the heme resonances (Fig. 3, *trace g*), thus providing further evidence for the nonreduction of ROO hemes in these conditions.

The previous experiment demonstrates spectroscopically the involvement of Rd in the reduction of ROO, but it does not rule out its possible participation as an effector. To clarify this issue, a set of experiments in which reduced rubredoxin was allowed to react with ROO was performed. Mixing anaerobically Rd with NADH and catalytic amounts of NRO results in complete reduction of Rd within minutes (Fig. 7, *inset*). When this reduced rubredoxin is added to ROO under anaerobic conditions (Fig. 7, *trace a*), reduction of the flavins occurs, as evaluated by the decrease in absorbance at 460 nm (Fig. 7, *trace b*). Simultaneously, Rd is reoxidized causing the appearance of a band at 490 nm. Similar experiments, performed using ascorbate reduced Rd and dithionite reduced Rd, without excess of reductant, also showed the reduction of ROO flavins (data not shown).

Genomic Organization: Rd and ROO Are Clustered in the Same Operon—Using a homologous probe prepared as described under "Experimental Procedures," several positive phage plaques were isolated from a genomic library of *D. gigas*. The isolated DNA was analyzed by restriction mapping and Southern blotting (results not shown), and the *Bam*HI fragments were subcloned and sequenced. Fig. 8*A* illustrates the genomic organization of Rd and ROO. As can be seen, both

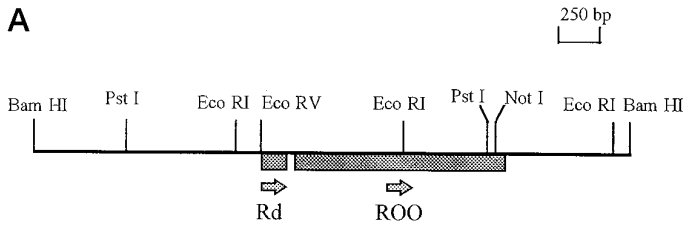

FIG. 8. **Partial restriction map and predicted amino acid sequences of Rd and ROO.** *Panel A*, partial restriction map of the subcloned 3.6-kilobase pair *Bam*HI-*Bam*HI DNA fragment. *Panel B*, amino acid sequence of Rd and the N terminus of ROO.

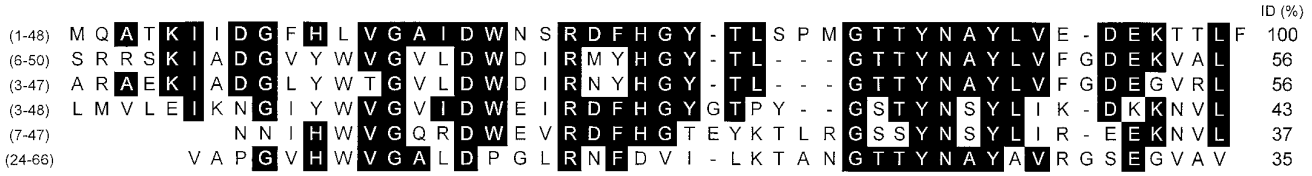

FIG. 9. **Sequence alignment of ROO N terminus with homologous proteins.** *D. gigas* rubredoxin:oxygen oxidoreductase (*Dg ROO*), *Methanococcus jannaschii* MJ0748 and MJ0732 products (*Mj MJ0748* and *Mj MJ0732*), *M. thermoautotrophicum* flavoprotein (*Mt fpaA*), *E. coli* ORF 0479 product (*Ec ORFo479*) and *R. capsulatus* ORFU1 product (*Rc ORFU1*). Between *parentheses* is the range of residues compared.

TABLE I
Comparison of properties from flavoheme proteins

Protein	Organism	Molecular mass	Cofactors	Function	Reference
		kDa			
Group I: Oxygen reactive flavoheme proteins					
Rubredoxin-oxygen oxidoreductase	*D. gigas*	86	FAD, mesoheme IX Fe-Uroporphyrin I	Terminal O_2 reductase	This work
Hemoglobin-like protein (Hmp)	*E. coli*	44	FAD, protoheme IX	O_2 sensor	34
Yeast hemoglobin	*Candida mycoderma*	50	FAD, protoheme IX	O_2 transport	35
Flavoheme protein	*Alcaligenes eutrophus*	43	FAD, protoheme IX		36
P-450 BM3	*Bacillus megaterium*	119	FAD, FMN, protoheme IX	Monooxygenase activity	38
Group II: Non-oxygen reactive flavoheme proteins					
Nitric oxide synthase	Mammalian	150	FAD, FMN, protoheme IX	NO synthase	39
Flavocytochrome b_2	*E. coli, Saccharomyces cerevisiae*	230	FMN, protoheme IX	L-Lactate dehydrogenase	40
Flavocytochrome *c*	*Chlorobium thiosulfatophilum*	57	FAD, mesoheme IX	Sulfide dehydrogenase	41
Flavocytochrome *c*	*Shewanella putrefaciens*	63.8	FAD, mesoheme IX	Fumarate reductase	42
Secondary amine monooxygenase	*Pseudomonas aminovorans*	210	Heme, Flavin and non-heme iron	Amine oxygenase	43

coding units are located in the same polycistronic unit. The sequences of Rd and the N-terminal end of ROO are identical to those obtained by chemical procedures (Fig. 8*B*).

Screening of protein sequence data bases revealed that the ROO N terminus shows high homologies toward a few proteins: two putative flavoproteins from *Methanococcus jannaschii* (31); a potential FMN-binding protein from *Rhodobacter capsulatus*, the product of the ORFU1 coding region (32); a flavoprotein from *Methanobacterium thermoautotrophicum* (33) and *E. coli* ORF o479 product, a not yet identified protein from *E. coli* (Fig. 9). In the case of the protein from *M. thermoautotrophicum*, toward which the ROO N-terminal end exhibits 56% identity, it is interesting to note that there is evidence for a rubredoxin being encoded in the same operon (33). Most striking is the finding of a block of seven residues which is conserved among these proteins: GTTYNAY. The sequence was compared against the Prosite motifs data bank; this block of residues was identified as a potential *N*-myristoylation site. However, since this block is internal to the sequence and ROO is most likely a fully processed protein, this possibility remains uncertain. Since most of the mentioned proteins contain flavin cofactors, the GTTYNAY sequence could represent a novel consensus motif for the binding of flavins.

DISCUSSION

D. gigas rubredoxin-oxygen oxidoreductase, in terms of its cofactors, may be considered as a member of the large superfamily of flavoheme proteins. From that large and heterogeneous family, two broad groups can be derived, based on their reactivity toward oxygen (Table I). Group I includes proteins that are directly involved in reacting or binding dioxygen. It comprises mainly the so-called flavohemoglobins, like the hemoglobin-like protein from *E. coli* (34). These soluble proteins have protoheme IX and FAD as cofactors and share domains from the globin and ferredoxin-$NADP^+$ reductase families (37). Their function is still uncertain, but they seem to play a role as oxygen sensors. Another member of this group is the cytochrome P-450 from *Bacillus megaterium* (P-450 BM3), which presents the unique feature of having in a single polypeptide chain both the heme and the flavin moieties (37). Group II includes the flavohemeproteins that are not reported to be reactive with oxygen and is somehow more heterogeneous in

TABLE II
Comparison of EPR properties of D. gigas ROO, cytochromes P-450, and other heme containing proteins

Protein	g_1	g_2	g_3	Reference
ROO (range of preparations)	2.39–2.47	2.26–2.32	1.88–1.92	This work
P-450 CAM	2.45	2.26	1.91	28
P-450 BM3	2.42	2.26	1.92	29
E. coli Hmp (cysteine derivative)	2.48	2.28	1.87	34
Mammalian NO synthase	2.44	2.29	1.89	39
Vitreoscilla bacterial hemoglobin	2.43	2.24	1.91	45

terms of size and cofactors of its elements. Very interestingly, a member of this group, the rat nitric oxide synthase, was shown to contain a FMN-binding domain which has a strong analogy with the flavodoxins from sulfate reducing bacteria (43). However, homologies between the N termini of the flavohemeproteins from both groups and the N terminus from ROO were not found. Nevertheless, the homology of this ROO partial sequence with some flavoproteins in such diverse organisms as methanogens and photosynthetic bacteria is surprising (Fig. 9). Unfortunately, the functions of these last proteins are not yet known.

The EPR features of ROO, namely the g values observed and the relaxation properties of the heme resonances, are strikingly similar to those of P-450 hemes (Table II), being so far observed only in cysteinyl coordinated hemes. It may then be proposed that one or both hemes in ROO are also coordinated to a cysteine residue. Also, the g value shift detected upon incubation with the ROO reductase system (NRO and Rd) is observed when P-450 is mixed with P-450 reductase (28). Interestingly, similar EPR signals were detected, with variable intensities depending on the preparation, for some of the flavohemeproteins presented in Table I, but these were not clearly assigned.

The reduction potentials of the flavin transitions (0 ± 15 and -130 ± 15 mV) are well in the range of what is found in flavoproteins (from -495 to $+80$ mV) (46). The fact that the electron donor is the one-electron carrier Rd leads necessarily to the formation of a stable semiquinone radical species.

Contrary to what is observed for the other flavohemeproteins from Group I, the reaction with oxygen in ROO appears to occur exclusively at the level of the flavins. However, in contrast to most of the oxidases containing flavins, ROO is not reduced by NADH. The low redox potential of ROO hemes (-350 ± 15 mV) when compared with those of the flavins (0 ± 15 mV and -130 ± 15 mV), together with the fact that they are neither reduced by NADH, NRO, and Rd, nor by reduced Rd, and the fact that this does not prevent catalytic activity, suggests that they are absent from reactivity with oxygen.

The coupling properties of some redox proteins from *D. gigas* with ROO were tested. However, as evaluated by EPR, mixing ROO under hydrogen with either hydrogenase and cytochrome c_3 or hydrogenase, cytochrome c_3, and the high molecular weight cytochrome does not result in heme reduction. Possibly, the hemes provide a second electron entry point to the enzyme through an unknown electron donor and/or are involved in an as yet undetermined catalytic reaction, such as enzymatic regulation.

Very interestingly, both coding units for Rd and ROO are clustered in the same operon (Fig. 8), indicating that they are under the same transcriptional control. In fact, it has been shown that proteins involved in the same metabolic pathway are organized as an operon (47, 48). This finding strongly reinforces the evidence obtained by spectroscopic analysis that reduced rubredoxin is directly involved in electron donation to ROO.

The determined redox potentials of ROO flavins are apparently in thermodynamic contradiction with the observations reported here according to which flavins are fully reduced by Rd, which has a reduction potential of ~0 mV. In fact, in the presence of the complete redox chain (NADH, NRO, Rd, and ROO), there is enough thermodynamic power to reduce the oxidase, but since reduced Rd can also reduce ROO flavins it may be suggested that the interaction of Rd with ROO causes a slight shift on the reduction potentials of either Rd or ROO flavins.

This is the first example for a rubredoxin function in sulfate reducing bacteria, despite the fact that they have been known and well characterized for a long time. Examples of physiological pathways in which a clear role for rubredoxin was found are scarce (51, 52). The best documented example so far is the multienzyme system in *Pseudomonads*, responsible for the metabolism of *n*-alkanes which is composed by NADH-rubredoxin oxidoreductase, rubredoxin, and a hydroxylase acting as a monooxygenase, found in the aerobe *Pseudomonas oleovorans* (52), a catalytic redox chain reminiscent of that operative in *D. gigas* for the reduction of dioxygen.

Acknowledgments—We are indebted to A. Mariano, P. Fareleira (Instituto de Tecnologia Química e Biológica (ITQB)), and L. Chen (University of Georgia) for their collaboration in the early stages of this work; M. Regalla (ITQB) for performing the N-terminal sequence; Prof. E. Melo (ITQB) for the collaboration in the fluorescence spectroscopy, and the staff of University of Georgia fermentation plant for growing the bacteria.

REFERENCES

1. Diling, W., and Cypionka, H. (1990) *FEMS Microbiol. Lett.* **71,** 123–128
2. Marschall, C., Frenzel, P., and Cypionka, H. (1993) *Arch. Microbiol.* **159,** 168–173
3. Santos, H., Fareleira, P., Xavier, A. V., Chen, L., Liu, M.-Y., and LeGall, J. (1995) *Biochem. Biophys. Res. Commun.* **195,** 551–557
4. LeGall, J., and Xavier, A. V. (1996) *Anaerobe* **2,** 1–9
5. Chen, L., Lui, M.-Y., LeGall, J., Liu, Fareleira, P., Santos, H., and Xavier, A. V. (1993) *Eur. J. Biochem.* **216,** 443–448
6. Moura, I., Moura J. J. G., Santos, M. H., Xavier, A. V., and LeGall, J. (1979) *FEBS Lett.* **107,** 419–421
7. Chen, L., Liu M.-Y., LeGall, J., Fareleira P., Santos, H., and Xavier, A. V. (1993) *Biochem. Biophys. Res. Commun.* **193,** 100–105
8. Moura, I., Bruschi, M., LeGall, J. Moura, J. J. G., and Xavier, A. V. (1977) *Biochem. Biophys. Res. Commun.* **75,** 1037–1044
9. Bruschi, M., Hatchikian, C. E., Golovleva, L. A., and Le Gall, J. (1977) *J. Bacteriol.* **129,** 30–38
10. Bruschi, M., and LeGall, J. (1972) *Biochim. Biophys. Acta* **263,** 279–282
11. Timkovich, R., Burkhalter, R. S., Xavier, A. V., Chen, L., and LeGall, J. (1994) *Bioorg. Chem.* **22,** 284–293
12. LeGall, J., Mazza, G., and Dragoni, N. (1965) *Biochim. Biophys. Acta* **99,** 385–387
13. Thoenes, U., Flores, O. L., Neves, A., Devreese, B., Van Beeumen, J. J., Huber, R., Romão, M. J., LeGall, J., and Rodrigues-Pousada, R. (1994) *Eur. J. Biochem.* **220,** 901–910
14. Ausubel, F. M., Brent, R., Kingston, R. E., Moore, D. D., Seidman, J. G., Smith, J. A., and Struhl, K. (1995) *Current Protocols in Molecular Biology,* Greene Publishing Associates and Wiley-Interscience, New York
15. Sambrook, J. Fritsch, E. F., and Maniatis, T. (1989) *Molecular Cloning: A Laboratory Manual,* 2nd Ed., Cold Spring Harbor Laboratory, Cold Spring Harbor, NY
16. Sigal, N., Senez, J. C., Le Gall, J., and Sebald, M. (1963) *J. Bacteriol.* **85,** 1315–1318
17. LeGall, J., and Dragoni, N. (1966) *Biochem. Biophys. Res. Commun.* **23,** 145–149
18. Bradford M. M. (1976) *Anal. Biochem.* **72,** 248–254
19. Teixeira, M., Batista, R., Gomes, C., Mendes, J., Pacheco, I., Anemuller, S., and Hagen, W. R. (1995) *Eur. J. Biochem.* **227,** 322–327
20. Aasa, R., and Vänngård, T. (1975) *J. Magn. Resonance* **19,** 308–315
21. Bolard, J., and Garnier, A. (1972) *Biochim. Biophys. Acta* **263,** 535–549
22. Henry, E. R., and Hofrichter, J. (1992) *Methods Enzymol.* **210,** 129–192
23. Massey, V., and Hemmerich, P. (1980) *Biochem. Soc. Trans.* **8,** 246–257
24. Calcaterra, N. B., Picó, G. A., Orellano, E. G., Ottado, J., Carrillo, N., and Ceccarelli, E. A. (1995) *Biochemistry* **34,** 12842–12848
25. Romero, A., Caldeira, J., LeGall, J., Moura, I., Moura, J. J. G., and Romão, M. J. (1996) *Eur. J. Biochem.* **239,** 190–196
26. Karplus, P. A., Daniels, M. J., and Herriot, J. R. (1991) *Science* **251,** 60–66
27. Lipscomb, J. D. (1980) *Biochemistry* **19,** 3590–3599
28. Dawson, J. H., Andersson, L. A., and Sono, M. (1982) *J. Biol. Chem.* **257,** 3606–3617
29. McKnight, J., Cheesman, M. R., Thomson, A. J., Miles, J. S., and Munro, A. W.

(1993) *Eur. J. Biochem.* **213,** 683–687
30. LeGall, J. (1968) *Ann. Inst. Pasteur (Paris)* **114,** 109–115
31. Bult, C. J., White, O., Olsen, G. J., Zhou, L., Fleischmann, R. D., Sutton, G. G., Blake, J. A., FitzGerald, L. M., Clayton, R. A., Gocayne, J. D., Kerlavage, A. R., Dougherty, B. A., Tomb, J. F., Adams, M. D., Reich, C. I., Overbeek, R., Kirkness, E. F., Weinstock, K. G., Merrick, J. M., Glodek, A., Scott, J. L., Geoghagen, N. S. M., Weidman, J. F., Fuhrmann, J. L., Nguven, D., Utterback, T. R., Kelly, J. M., Peterson, J. D., Sadow, P. W., Hanna, M. C., Cotton, M. D., Roberts, K. M., Hurst, M. A., Kaine, B. P., Borodovsky, M., Klenk, H. P., Fraser, C. M., Smith, H. O., Woese, C. R., and Venter, J. C. (1996) *Science* **273,** 1058–1073
32. Saeki, K., Tokuda, K., Fujiwara, T., and Matsubara, H. (1993) *Plant Cell Physiol.* **34,** 185–199
33. Nölling, J., Ishii, M., Kock, J., Pihl, T., Reeve, J., Thauer, R., and Hedderich, R. (1995) *Eur. J. Biochem.* **231,** 628–638
34. Ioannidis, N., Cooper, C. E., and Poole, R. K. (1992) *Biochem. J.* **288,** 649–655
35. Oshino, R., Asakura, T., Takio, K., Oshino, N., and Chance, B. (1973) *Eur. J. Biochem.* **39,** 581–590
36. Probst, I., Wolf, G., and Schlegel, H. G. (1979) *Biochim. Biophys. Acta* **576,** 471–478
37. Narhi, L. O., and Fulco, A. J. (1986) *J. Biol. Chem.* **261,** 7160–7169
38. Porter, T. D. (1991) *Trends Biochem. Sci.* **16,** 154–158
39. Stuehr, D. J., and Ikeda-Saito, M. (1992) *J. Biol. Chem.* **267,** 20547–20550
40. Black, M. T., White, S. A., Reid, G. A., and Chapman, S. K. (1989) *Biochem. J.* **258,** 255–259
41. Van Beeumen, J. J., Demol, H., Samyn, B., Bartsch, R. G., Meyer, T. E., Dolata, M. M., and Cusanovitch, M. A. (1990) *J. Biol. Chem.* **266,** 12921–12931
42. Morris, C. J., Black, A. C., Pealing, S. L., Manson, F. D. C., Chapman, S. K., Reid, G. A., Gibson, D. M., and Ward, F. B. (1994) *Biochem. J.* **302,** 587–593
43. Alberta, J. A., Andersson, L. A., and Dawson, J. H. (1989) *J. Biol. Chem.* **264,** 20467–20473
44. Deleted in proof
45. Kroneck, P. M., Jakob, W., Webster, D. A., and DeMaio, R. (1991) *Biol. Metals* **4,** 119–125
46. Cooper, C. E., Ioannidis, N., D'Mello, R., and Poole, R. K. (1994) *Bioch. Soc. Trans.* **22,** 709–713
47. Nielsen, A. K., Gerdes, K., Degn, H., and Murrel, J. C. (1996) *Microbioloby* **142,** 1289–1296
48. Yamazaki, M., Thorne, L., Mikolajczak, M., Armentrout, R. W., and Pollock, T. J. (1996) *J. Bacteriol.* **178,** 2676–2687
49. Tegoni, M., Janot, J. M., and Labeyrie, F. (1986) *Eur. J. Biochem.* **155,** 491–503
50. Deleted in proof
51. Ragsdale, S. W., Ljungdahl, L. G., and DerVartanian, D. V. (1983) *J. Bacteriol.* **155,** 1224–1237
52. Ruettinger, R. T., Griffith, G. R., and Coon, M. J. (1977) *Arch. Biochem. Biophys.* **183,** 528–537